

## Synthesis and Liquid Crystalline Behavior of Laterally Substituted Polyimides with Siloxane Linkages

Yu Shoji, Ryohei Ishige, Tomoya Higashihara, Susumu Kawauchi, Junji Watanabe, and Mitsuru Ueda\*

*Department of Organic and Polymeric Materials, Graduate School of Science and Engineering, Tokyo Institute of Technology, 2-12-1-H-120, O-okayama, Meguro-Ku, Tokyo 152-8552, Japan*

*Received August 1, 2010; Revised Manuscript Received September 13, 2010*

**ABSTRACT:** Novel siloxane-containing liquid crystalline (LC) polyimides with methyl, chloro, and fluoro substituents on mesogenic units have been developed from siloxane-containing diamines with pyromellitic dianhydride (PMDA) or 3,3',4,4'-tetracarboxybiphenyl dianhydride (BPDA), and their thermotropic LC behavior was examined. Among these, chloro and fluoro substituents are effective for the formation of LC phases, particularly when those are substituted away from the center of the mesogenic unit: the isotropization temperature is not much affected, but the crystal–LC transition temperatures are significantly decreased. On the other hand, the methyl substituent tends to interrupt liquid crystallization as well as crystallization. Thus, the fluoro-substituted polyimide derived from BPDA exhibited the lowest crystalline–LC transition temperature ( $T_{cr-lc} = 134$  °C) among all polyimides, showing a wide liquid crystal temperature up to 238 °C. From the X-ray diffraction measurement conducted for the oriented mesophases of fibrous polyimides, they were found to form SmA and SmC as high- and low-temperature mesophases, respectively.

### Introduction

Insulating polymers with high thermal conductivity have recently been shown to be attractive materials for effectively releasing generated heat from densely packaged electronics devices. Since organic polymeric materials are generally thermal insulators, the development of low dielectric and thermoconductive polymers are required at the present time. Liquid crystalline (LC) polymers are expected to increase thermal conductivity because the alignment of LC polymers effectively conducts “phonon” which is the media of thermal conductivity for organic polymers.<sup>1</sup> Furthermore, the direction of phonon conductivity corresponds to the alignment of polymer main chains, and such alignment can easily be controlled in common ways, for example, by stretching, rubbing, magnetic fields, self-alignment, and so on.<sup>1–6</sup>

There are two requirements for thermal conductive materials used in practical applications. One is solution processability, and the other is low transition temperatures of LC polymers to decrease the processing temperature. Aromatic polyimides should be applicable as thermal conductive materials because the precursors polyimides, which are poly(amic acid)s, have the advantage of solution processability, although most polyimides are generally insoluble. However, only a few LC polyimides have so far been reported, such as wholly aromatic and thermotropic LC polyimides with methylene or oxyethylene units.<sup>7–11</sup> In a preceding work, we reported the synthesis of thermotropic LC polyimides from diamines containing siloxane spacer units and pyromellitic dianhydride (PMDA) or 3,3',4,4'-tetracarboxybiphenyl dianhydride (BPDA).<sup>12,13</sup> The crystal–LC transition temperatures ranged from 222 to 275 °C in the heating process, depending on the number of methylene or siloxane units. These LC transition temperatures were lower than those of corresponding polyimides with alkylene or oxyethylene spacer units. However,

a further decrease in the transition temperatures of polyimides is required to avoid the destruction of semiconductor chips inside integrated circuits (ICs) during the fabrication process in practical application. Although methyl-substituted polyimides were synthesized by aiming at twisting the coplanar imide rings and loosening the packing of the mesogens to decrease their transition temperatures, they unfortunately did not show liquid crystallinity.

In this report, we describe the synthesis of novel laterally substituted LC polyimides derived from PMDA or BPDA with diamines containing siloxane spacer units and their thermotropic LC behavior in detail. The purpose of this work is to determine which kinds and positions of substituents are effective for decreasing the crystal–LC transition temperatures of polyimides. The molecular designs of the substituents include methyl, fluoro, and chloro groups, expected to reduce the molecular interaction of the mesogenic units.

### Results and Discussion

An LC polyimide backbone with octamethyltetrasiloxane spacer units was selected, which showed the lowest crystal–LC transition temperature (222 °C) in a previous work.<sup>13</sup> Methyl-, fluoro-, or chloro-substituted diamine monomers containing octamethyltetrasiloxane units (**3b–d**, **3f**) were newly synthesized under standard conditions for Williamson's ether synthesis, hydrosilylation, and reduction, as shown in Scheme 1.

Figure 1 representatively shows the <sup>1</sup>H and <sup>13</sup>C NMR spectra for diamine **3d** in CDCl<sub>3</sub>. The signal assignments in the <sup>1</sup>H NMR spectrum of **3d** are consistent with the proposed structures. The signals at 6.53 (b) and 6.76 ppm (a, c) correspond to aromatic protons. The resonances for methylene protons (g, f, e, and d) were clearly observed at 0.57–0.63, 1.47–1.58, 1.76–1.85, and 3.93 ppm, respectively. Furthermore, the signals of protons adjacent to the methylsilyl groups appeared at 0.05 and 0.08 ppm. The target structure of **3d** was also confirmed from the <sup>13</sup>C NMR spectrum, showing the expected 12 signals.

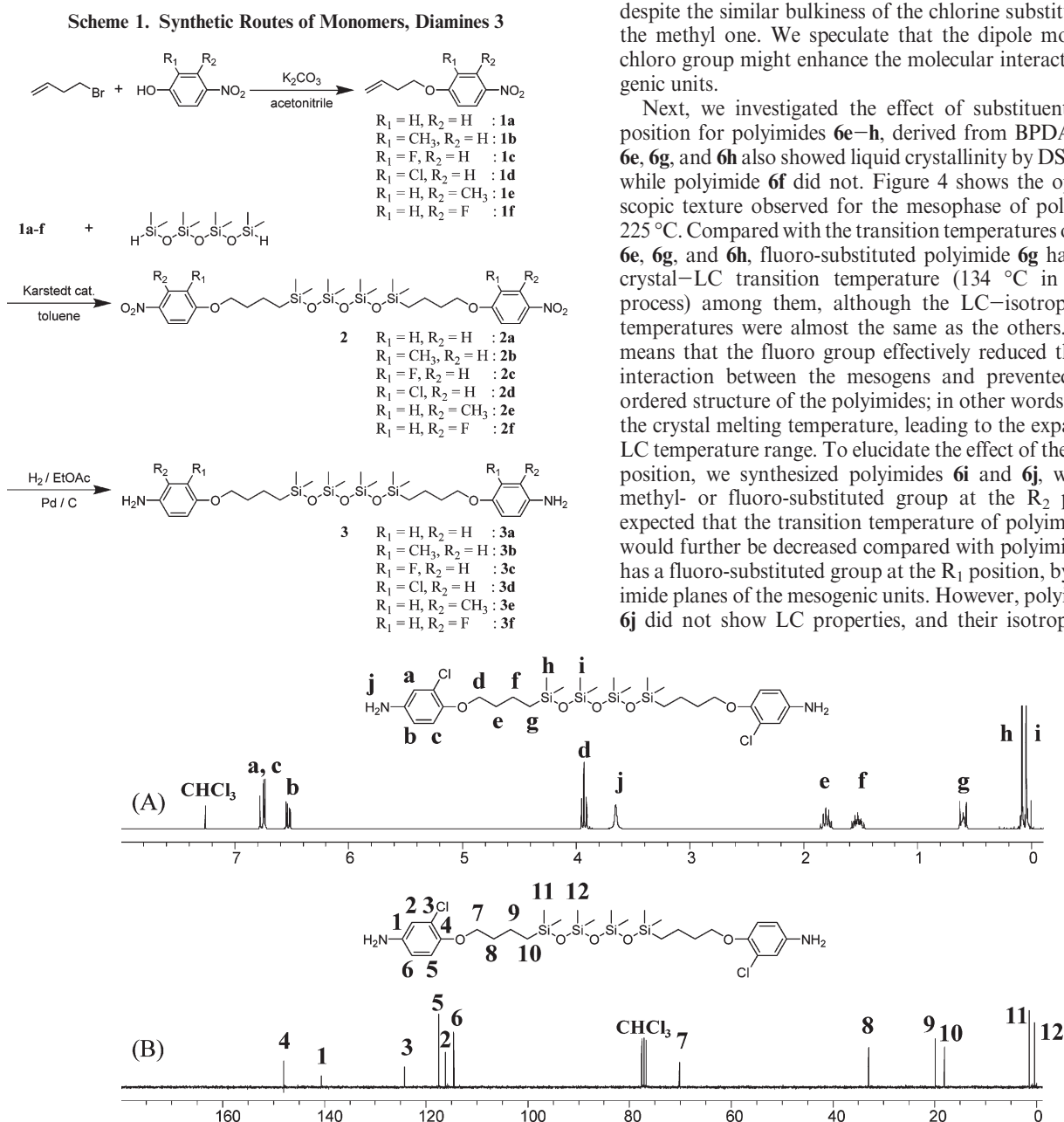
\*Corresponding author. E-mail: mueda@polymer.titech.ac.jp.

Polyimides **6** were synthesized by using a two-step polycondensation procedure, as shown in Scheme 2. Poly(amic acid)s (PAAs), which are the precursors of polyimides, were prepared from each diamine **3** and tetracarboxydianhydride derivatives (PMDA (**4a**) or BPDA (**4b**)) at room temperature in *N*-methylpyrrolidone (NMP). The resulting PAAs had high inherent viscosities in the range 0.62–2.04 dL/g (Table 1). Then they were cast and gradually heated up to 200 °C for 2 h on glass substrates under nitrogen to obtain polyimide films. In the representative FT-IR spectrum of prepared polyimide **6g**, the peaks for the amic acid groups disappeared and the characteristic imide peaks at 1770 (C=O asymmetric stretching), 1713 (C=O symmetric stretching), and 1389 cm<sup>-1</sup> (C–N stretching) appeared, indicating complete imidization. The expected polyimide structures were also confirmed by elemental analysis.

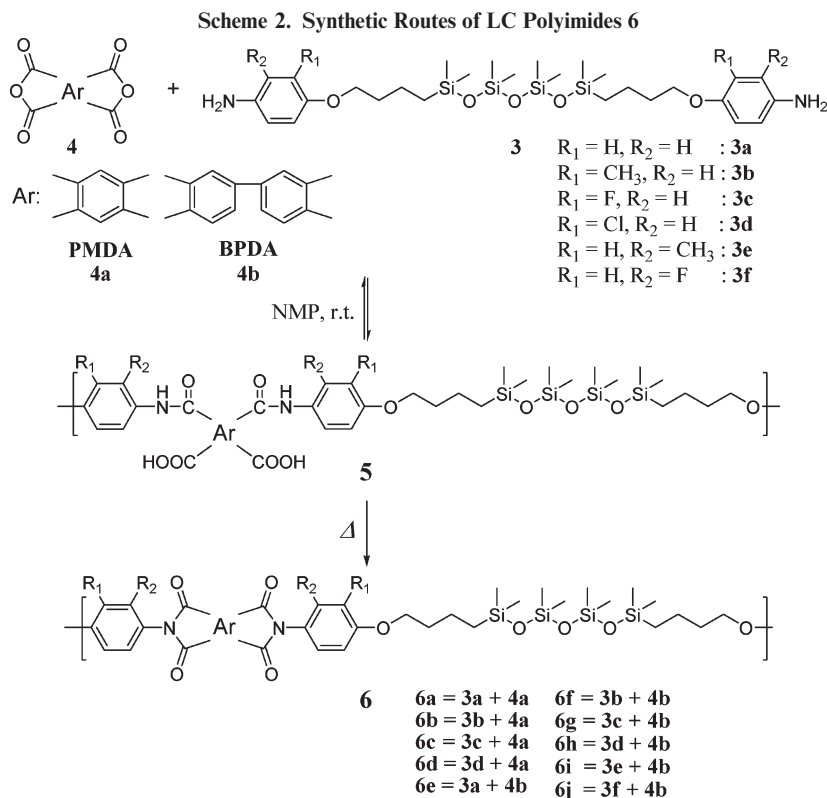
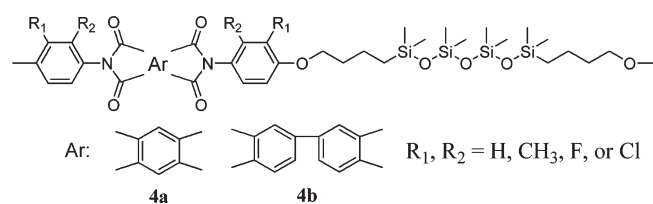
All polyimides **6** possess high thermal stability over 440 °C ( $T_{d5\%}$ ) according to thermogravimetric analysis (TGA) under nitrogen (Table 1). The differential scanning calorimetry (DSC)

curves of all polyimides **6** are shown in Figure 2. The crystal melting temperatures in polyimides **6** were 237 (**6a**), 197 (**6b**), 237 (**6c**), 242 (**6d**), 222 (**6e**), 193 (**6f**), 163 (**6g**), 186 (**6h**), and 210 °C (**6j**) (Table 2, Figure 3), while polyimide **6i** showed an amorphous nature. Polyimides **6a** and **6c** derived from PMDA showed more than two exothermic peaks in the cooling process. In addition, birefringence and fluidity were observed in the temperature range between these peaks by polarizing optical microscopy (POM). Therefore, the phase between the transition temperatures corresponds to the liquid crystalline phase. On the other hand, the methyl- or chloro-substituted polyimides, **6b** and **6d**, did not show the liquid crystallinity according to DSC trace and POM. With respect to the melting points of the polyimides derived from PMDA, there was no noticeable change among polyimides **6a**, **6c**, and **6d**. Only methyl-substituted polyimide **6b** had the lowest melting point among them, probably because the molecular interaction was reduced by a bulky substituent. The melting point of chloro-substituted polyimide **6d** was almost the same as nonsubstituted polyimide **6a** and fluoro-substituted **6c**, despite the similar bulkiness of the chlorine substituent of **6d** to the methyl one. We speculate that the dipole moment of the chloro group might enhance the molecular interaction of mesogenic units.

Next, we investigated the effect of substituents at the R<sub>1</sub> position for polyimides **6e–h**, derived from BPDA. Polyimides **6e**, **6g**, and **6h** also showed liquid crystallinity by DSC and POM, while polyimide **6f** did not. Figure 4 shows the optical microscopic texture observed for the mesophase of polyimide **6h** at 225 °C. Compared with the transition temperatures of polyimides **6e**, **6g**, and **6h**, fluoro-substituted polyimide **6g** had the lowest crystal–LC transition temperature (134 °C in the cooling process) among them, although the LC–isotropic transition temperatures were almost the same as the others. It probably means that the fluoro group effectively reduced the molecular interaction between the mesogens and prevented the highly ordered structure of the polyimides; in other words, it decreased the crystal melting temperature, leading to the expansion of the LC temperature range. To elucidate the effect of the substitution position, we synthesized polyimides **6i** and **6j**, which have a methyl- or fluoro-substituted group at the R<sub>2</sub> position and expected that the transition temperature of polyimide **6i** and **6j** would further be decreased compared with polyimide **6g**, which has a fluoro-substituted group at the R<sub>1</sub> position, by twisting the imide planes of the mesogenic units. However, polyimides **6i** and **6j** did not show LC properties, and their isotropic transition



**Figure 1.** (A) <sup>1</sup>H and (B) <sup>13</sup>C NMR spectra of the diamine **3d**.

**Table 1. Polymerization Results and Thermal Stabilities**

polymer	Ar	R <sub>1</sub>	R <sub>2</sub>	$\eta_{\text{inh}}$ [dL/g] <sup>a</sup>	$T_{\text{d}1\%}$ [°C] <sup>b</sup>	$T_{\text{d}5\%}$ [°C] <sup>b</sup>
<b>6a</b>	<b>4a</b>	H	H	0.66	415	455
<b>6b</b>	<b>4a</b>	CH <sub>3</sub>	H	0.67	421	443
<b>6c</b>	<b>4a</b>	F	H	0.62	412	443
<b>6d</b>	<b>4a</b>	Cl	H	0.86	414	444
<b>6e</b>	<b>4b</b>	H	H	1.43	430	457
<b>6f</b>	<b>4b</b>	CH <sub>3</sub>	H	2.04	415	443
<b>6g</b>	<b>4b</b>	F	H	0.83	426	443
<b>6h</b>	<b>4b</b>	Cl	H	0.75	420	446
<b>6i</b>	<b>4b</b>	H	CH <sub>3</sub>	0.78	408	452
<b>6j</b>	<b>4b</b>	H	F	1.60	392	440

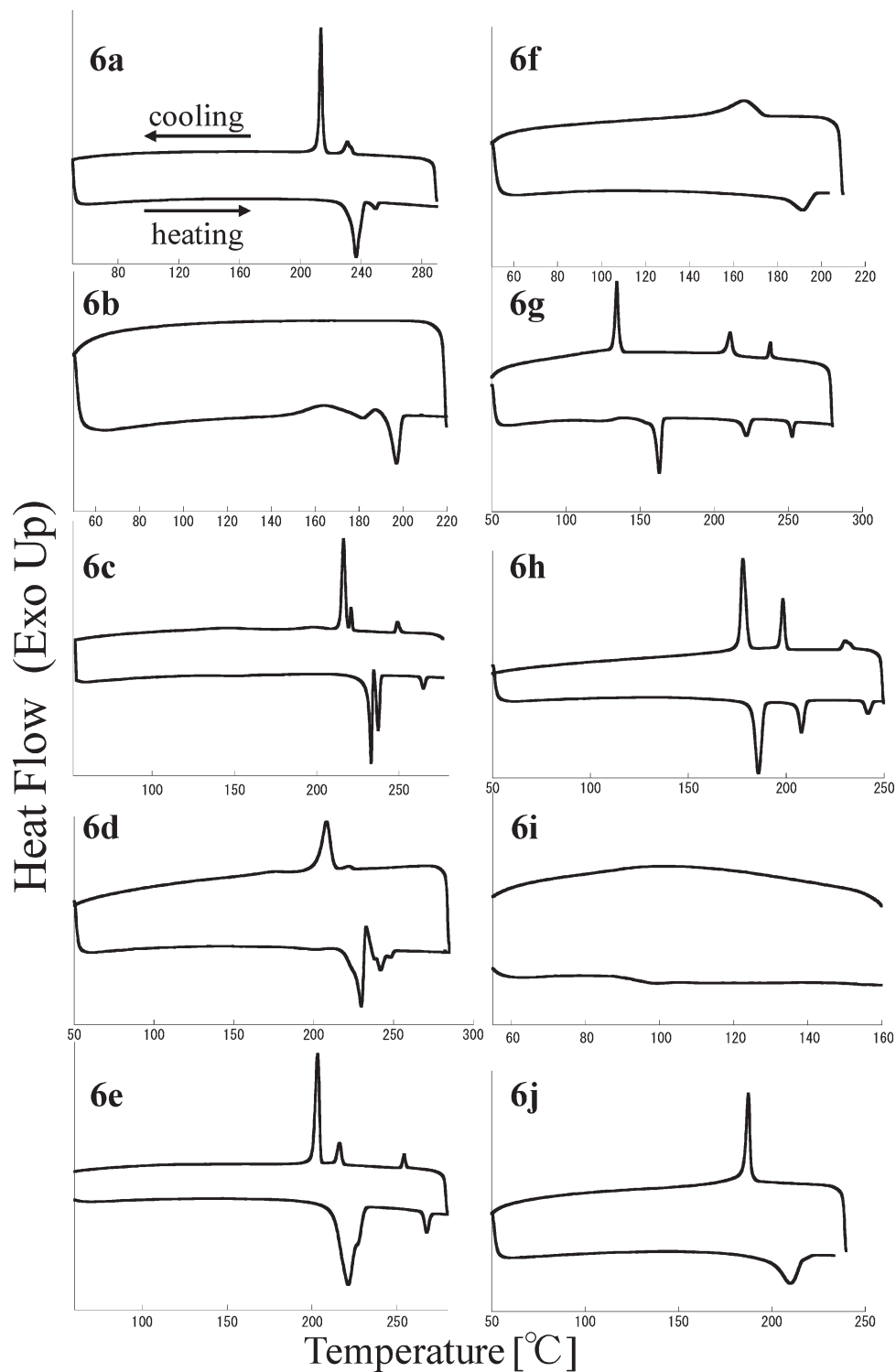
<sup>a</sup>Inherent viscosities were measured at 30 °C in NMP at a PAA 5 concentration of 0.5 g/dL. <sup>b</sup>Decomposition temperature.  $T_{\text{d}1\%}$ : 1% weight loss temperature,  $T_{\text{d}5\%}$ : 5% weight loss temperature.

temperatures decreased. This is probably because the methyl or fluoro substitution at the R<sub>2</sub> position twisted the imide plane and led to a significant decrease in the molecular interaction of the mesogenic units, destabilizing the crystalline phase or mesophase. To support this result, molecular simulation of the mesogenic units of polyimides **6e**, **6g**, and **6j** was carried out by density functional theory. The equilibrium structures of those polyimides were optimized and verified by frequency analysis at B3LYP/6-3/G(d) (Figure 5). The dihedral angle of the phenyl and imide groups for polyimide **6j** was 58.1°, which was wider than 42.7° for polyimide **6e** and 39.9° for polyimide **6g**. These results are similar to a previous report, wherein Coates suggested that a lateral

substituent is the most efficient for producing a smectic C phase when it is substituted away from the center of the mesogen molecule and has reduced the occurrence of higher-ordered phases.<sup>14</sup> In our results, the fluoro group at the R<sub>1</sub> position was also the most effective substituent for decreasing the crystal–LC transition temperatures; in other words, the fluoro substituent properly destabilized the crystalline phase. Consequently, the fluoro or chloro substitutions at the R<sub>1</sub> position of polyimides **6** from BPDA reduce the crystal–LC transition temperatures almost without changing their LC–isotropic transition temperatures, while the substitutions at the R<sub>2</sub> position reduce the isotropic transition temperatures for destabilizing the crystalline or LC phase. There is no clear explanation for the reason why the methyl-substituted polyimide **6i** derived from BPDA exceptionally shows an amorphous nature.

From optical microscopic observation of the fanlike texture, all the liquid crystals formed are smectic phase. X-ray diffraction observation also identifies the smectic phase, showing an outer broad hallow and inner sharp reflections. For polyimides **6c**, **6e**, **6g**, and **6h**, forming two mesophases, the higher temperature mesophase is the SmA and the lower temperature mesophase is the SmC. The layer spacings of the SmA and SmC phases are listed in Table 2. The SmA layer spacings (32.7–33.3 Å) of **6a** and **6c** are relatively smaller than those (35.4–35.9 Å) of **6e**, **6g**, and **6h**, reflecting the difference in length in the central unit of the mesogenic group.

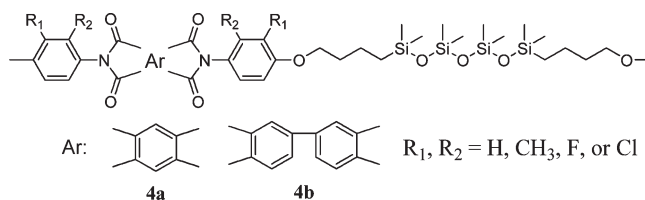
The detailed structural change in the SmA–SmC transition was investigated by wide-angle X-ray diffraction (WAXD) measurement in polyimide **6g**, which forms enantiotropic mesophases in the widest temperature range. To obtain a uniaxial orientation of the mesophases, the fiber was spun from isotropic melt at 280 °C. Figure 6a shows a typical WAXD pattern observed in a low-temperature liquid-crystal phase (180 °C in the heating process). Here, the fiber axis is set in the vertical direction. In a small-angle region of the fiber pattern (see enlarged view of small-angle region of Figure 6a), sharp layer reflections split on the left



**Figure 2.** DSC heating and cooling curves of polyimides **6** by the measurement performed at a scanning rate of 10 °C/min.

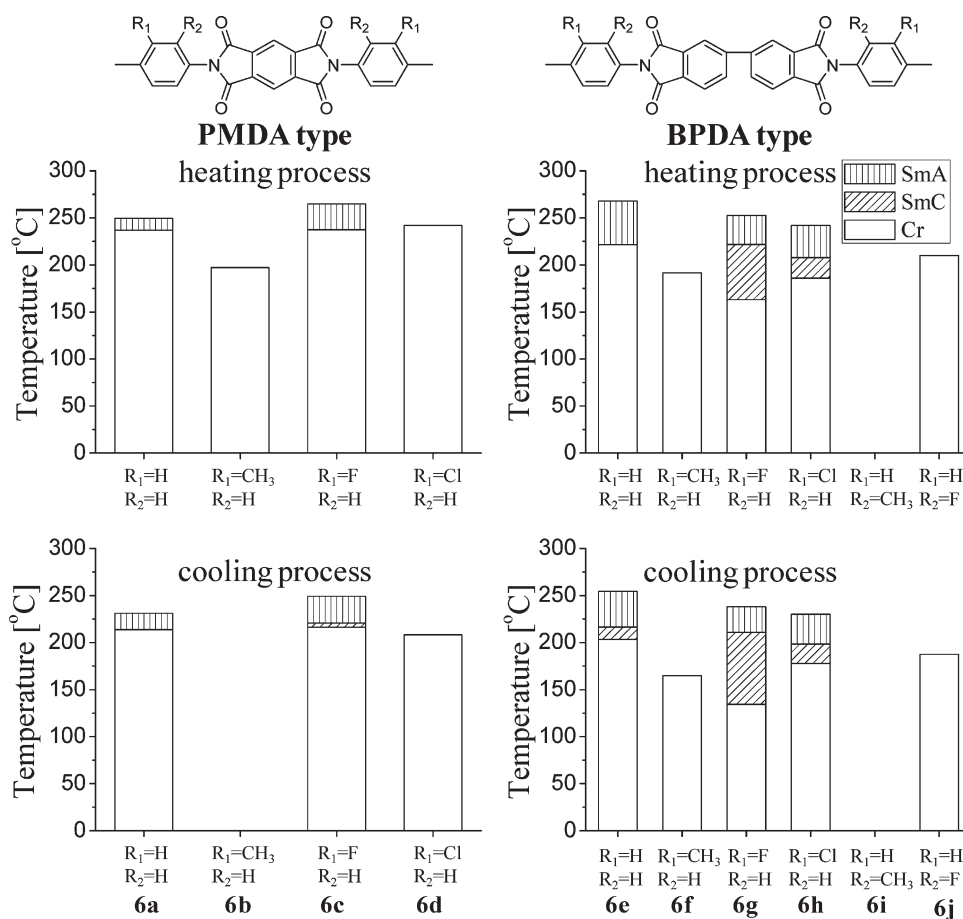
and right side of the meridian are observed. The spacing is 31.1 Å. On the other hand, an outer broad reflection with a spacing of 5.5 Å can be found on the equator. This diffraction profile gives just the luminescence of the SmC structure with the polymer chains lying parallel to the fiber axis and the layers normal tilted from the fiber axis.<sup>15</sup> Figure 6b shows the fiber pattern obtained for a high-temperature phase at 235 °C. This pattern has sharp reflections of the smectic layer on the meridian at 35.4 Å in the small-angle region and broad outer reflections whose intensity peak is on the equator at 6.6 Å. The orthogonal relationship between the layer reflection and outer broad reflection indicates

that this high-temperature phase is the SmA phase followed by SmC–SmA transition. In Figure 7, the tilt angle of the layer corresponding to the split angle  $\mu$  of the layer reflections is plotted against temperature. Of interest is that the tilt angle is somewhat independent of the SmC temperature and becomes zero discontinuously at the SmC–SmA transition, showing that the transition is of the first order. From a comparison of the spacing between the SmC and SmA phases, we can estimate a tilt angle of 30° under the assumption that the repeating unit length is maintained throughout the transition. This value is nearly equal to the observed one of 29°.

**Table 2. Thermal Transition Temperatures of Polyimides 6**

polymer	Ar	R <sub>1</sub>	R <sub>2</sub>	T <sub>m</sub> [°C] <sup>a</sup>	T <sub>cr-lc</sub> [°C] <sup>b</sup>	T <sub>lc-lc</sub> [°C] <sup>b</sup>	T <sub>lc-i</sub> [°C] <sup>b</sup>	ΔH [kJ mol <sup>-1</sup> ] <sup>b</sup>			d <sub>LC1</sub> [Å]	d <sub>LC2</sub> [Å]	tilt angle <sup>f</sup> [deg]
								lc-cr	lc-lc	iso-lc			
<b>6a</b>	<b>4a</b>	H	H	237	214	c	231	16.2		2.7		32.7	
<b>6b</b>	<b>4a</b>	CH <sub>3</sub>	H	197	d	d	d						
<b>6c</b>	<b>4a</b>	F	H	237	216	221	249	10.9	1.3	1.5		33.3	
<b>6d</b>	<b>4a</b>	Cl	H	242	d	d	d						
<b>6e</b>	<b>4b</b>	H	H	222	203	216	254	20.8	4.3	1.7	32.6	35.9	24
<b>6f</b>	<b>4b</b>	CH <sub>3</sub>	H	192	d	d	d						
<b>6g</b>	<b>4b</b>	F	H	163	134	211	238	8.6	4.5	1.4	31.1	35.4	29
<b>6h</b>	<b>4b</b>	Cl	H	186	178	198	230	13.5	5.4	1.7	32.2	35.4	36
<b>6i</b>	<b>4b</b>	H	CH <sub>3</sub>	e	e	e	e						
<b>6j</b>	<b>4b</b>	H	F	210	d	d	d						

<sup>a</sup>Melting points of polyimides **6** on the heating process. <sup>b</sup>Transition temperatures were determined as those at peak tops by DSC during a cooling scan at 10 °C/min. T<sub>cr-lc</sub>: crystal-LC transition temperature; T<sub>lc-lc</sub>: LC-LC transition temperature; T<sub>lc-i</sub>: LC-isotropic transition temperature. <sup>c</sup>No detection of LC-LC transition temperature. <sup>d</sup>There are no LC phases. <sup>e</sup>Amorphous nature. <sup>f</sup>These tilt angles were measured from the splitting angle of inner layer reflections in oriented X-ray patterns taken for the fibrous SmC phases (refer to Figure 6a).

**Figure 3.** Comparison of mesomorphic properties for polyimides **6**.

Although the SmA-SmC transformation is thus obvious, the present SmC and SmA phases possess some unusual structural features. First, the SmC phase shows a few of broad reflections along unusual directions in addition to the ordinal equatorial one

with a spacing of 5.5 Å, that is, 6.4 and 5.0 Å ones along the meridional and off-meridional directions (see Figure 6a). This unusual pattern may be attributable to the formation of a two-dimensional pseudolattice; the strong segregation takes place

between the alkyl spacer part and dimethylsiloxane part,<sup>16</sup> giving a rise to short-range positional order along the layer plane direction. A second unusual feature is observed also on the broad outer reflection profile of the SmA phase. Irrespective of the high orientation of the layer, as can be found from the sharp inner reflection concentrated on the meridian, the outer reflection is widely spread along the azimuthal direction. From the intensity profile of the outer broad reflection along the azimuthal direction, in fact, the orientational order parameter  $\langle P_2 \rangle$  of the mesogenic part is evaluated as 0.4. This low orientational order reminds us of the “de Vries” type of SmA phase, in which the mesogens are significantly tilted to the layer normal, but their average axis is perpendicular to the layer. The average tilt angle is estimated as  $37^\circ$  from the layer normal. A third feature is the first-order SmA–SmC transition. Usually, the SmC–SmA phase transition is second-order, and the tilt angle changes continuously following the equation<sup>15</sup>  $(T_C - T)^{1/2}$ . In this case, however, the tilt angle changes discontinuously. The clear endothermic peak of the SmC–SmA transition observed on DSC thermograms on both

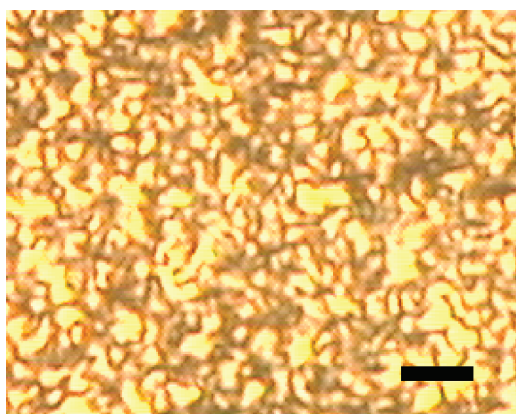


**Figure 4.** Polarized optical microscopic texture observed for SmC of polyimide **6h** at 225 °C (the scale bar indicates 25  $\mu\text{m}$ ).

the heating and cooling scan also supports that the transition is first-order. The first-transition behavior of the SmC–SmA transition has been predicted by Saunders et al. using a generalized theoretical Landau–de Gennes model.<sup>17–19</sup> As pointed out by Saunders, the fact that all known de Vries material does not form the nematic phase implies that the formation of the SmC phase is driven by an increase in the layering rather than orientation as the temperature decreases. In fact, our synthesized polyimide has a dimethylsiloxane group in the spacer which will be strongly segregated from the alkyl chains and aromatic mesogens, and this strong segregation is considered as a driving force to form the LC phase. Detailed structural analyses are now being carried out.

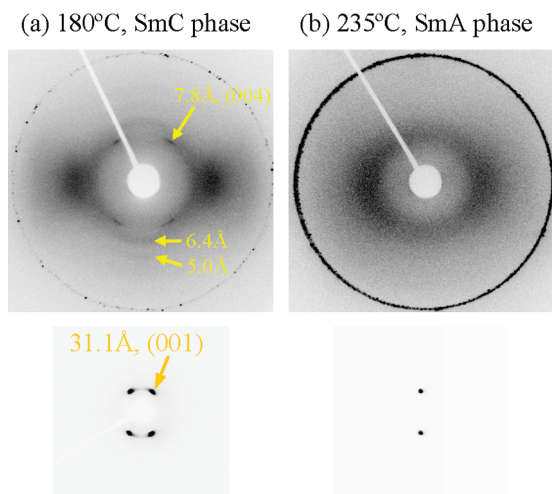


**Figure 6.** Wide-angle X-ray diffraction patterns of (a) SmC and (b) SmA phases observed in the fiber samples of **6g**. To show the smectic layer reflection, patterns in small-angle region are enlarged in the lower photographs. Fiber axis is set in a vertical direction.

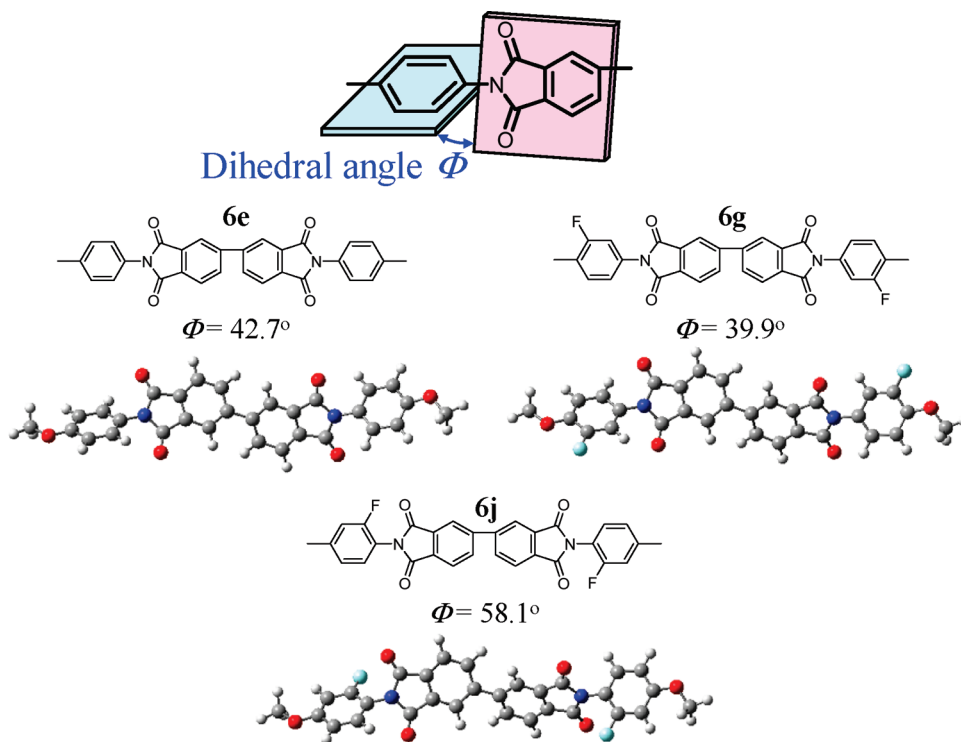


**Figure 5.** Optimized geometries of the mesogenic units of polyimides **6e**, **6g**, and **6j**.

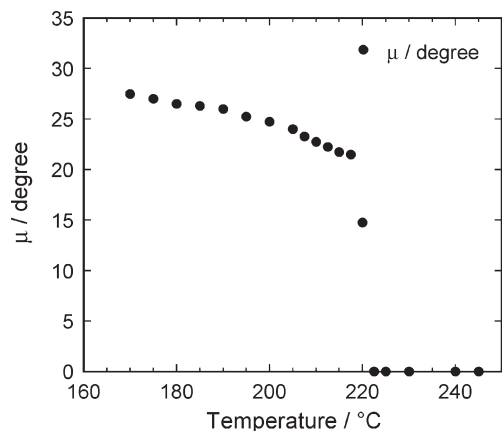


**Figure 7.** Tilt angle of the layer estimated from the split angle  $\mu$  of the layer reflection in WAXD fiber pattern is plotted against temperature.

### Conclusion

We have synthesized a new series of laterally substituted LC semialiphatic polyimides containing siloxane spacer units which showed high thermal stability ( $T_{d5\%} > \sim 450$  °C). Among the methyl, chloro, and fluoro substituents, the fluoro substituent was the most effective in stabilizing the liquid crystal phase: it reduces the crystal melting temperature substantially, but not the isotropization temperature of LC. The chloro substituent was found to be effective as well, but the methyl substituent, irrespective of being the same size as the chloro one, substantially destabilizes the LC phase. We have also been concerned with the position of the substituent. The  $R_1$  position, apart from the central part of the mesogen, was more effective than the  $R_2$  position. The liquid crystals formed are the SmA and SmC phases, as found from the oriented X-ray patterns taken for the fibrous samples. The structural features of these phases and the SmA–SmC transition behavior were observed especially for the fluoro substituent polyimide based on BPDA, **6g** showing the widest LC temperature region. Of interest is that an anomalous diffraction profile is observed on the outer broad reflection both in the SmA and SmC phases, although inner layer reflections are observed ordinarily in the meridional direction. In the SmC phases, some other broad reflections appear along the meridional direction in addition to the ordinary equatorial one and in the SmA phase; the broad reflection is significantly spread along the azimuthal direction irrespective of the high orientation of the layer. Further, these features are considered to be caused by the segregation of the siloxane group from the other moieties in the polymer chain, which will be examined in more detail in the near future.

### Experimental Section

**Measurement.** FT-IR spectra were measured on a Horiba FT-720 spectrometer.  $^1\text{H}$  and  $^{13}\text{C}$  NMR spectra were recorded with a Bruker DPX300S spectrometer. Inherent viscosities were measured at 30 °C in *N*-methylpyrrolidinone (NMP) at a polymer concentration of 0.5 g/dL. The transition characteristics were surveyed with a polarizing microscope (Olympus BX51), together with the use of a LINKAM LTS-350 hot stage equipped with a temperature controller by setting a polyimide film between crossed polarizers. Thermal analysis was performed on a Seiko EXSTAR 6000 TG/DTA 6300 thermal analyzer at a heating rate of 10 °C/min for thermogravimetry (TG) and a Perkin-Elmer DSC7 calorimeter connected to a cooling system at a heating rate of 10 °C/min for differential

scanning calorimetry (DSC). WAXD measurements were performed at ambient temperature by using a Rigaku-Denki RINT-2500 X-ray generator with monochromic Cu K $\alpha$  radiation (40 kV, 50 mA) from graphite crystal of monochromator and flat-plate type of imaging plate. Density functional theory calculations were carried out by using Gaussian09 program on TSUBAME supercomputer.

**Materials.** PMDA and BPDA were purified by sublimation prior to use. NMP, acetonitrile, and toluene were purified by distillation. Other reagents and solvents were purchased from TCI, Japan. The syntheses of diamine monomers **3a** and **3e** as well as polyimides **6a**, **6e**, and **6i** were described in the previous report.<sup>7</sup>

**General Synthesis for Diamines and Polymers.** The substituted diamine monomers **3** containing siloxane linkages were synthesized according to the previous report<sup>7</sup> under the standard conditions for Williamson's ether synthesis, hydrosilylation, and reduction. Polyimides were synthesized from PMDA or BPDA with diamines **3** by the solution polymerization in NMP followed by thermal imidization. Detailed synthesis and characterization of individual diamines **3** and polyimides **6** are described in the Supporting Information.

**Acknowledgment.** The financial support from Mitsubishi Chemical Corporation is gratefully acknowledged.

**Supporting Information Available:** Text giving experimental details about the synthesis and characterization of **1b–1d**, **1f**, **2b–2d**, **2f**, **3b–3d**, **3f**, **6b–6d**, **6f–6h**, and **6j** and Figure S1 showing the X-ray patterns of oriented polyimides **6a**, **6c**, **6e**, and **6h**. This material is available free of charge via the Internet at <http://pubs.acs.org>.

### References and Notes

- (1) Akatsuka, M.; Takezawa, Y. *J. Appl. Polym. Sci.* **2003**, *89*, 2464–2467.
- (2) Osada, K.; Niwano, H.; Tokita, M.; Kawauchi, S.; Watanabe, J. *Macromolecules* **2000**, *33*, 7420–7425.
- (3) Patil, H. P.; Lentz, D. M.; Hedden, R. C. *Macromolecules* **2009**, *42*, 3525–3531.
- (4) Kato, T.; Nagahara, T.; Agari, Y.; Ochi, M. *J. Polym. Sci., Part B* **2006**, *44*, 1419–1425.
- (5) Kato, T.; Nagahara, T.; Agari, Y.; Ochi, M. *J. Appl. Polym. Sci.* **2007**, *104*, 3453–3458.
- (6) Harada, M.; Ochi, M.; Tobita, M.; Kimura, T.; Ishigaki, T.; Shimayama, N.; Aoki, H. *J. Polym. Sci., Part B: Polym. Phys.* **2003**, *41*, 1739–1743.
- (7) Inoue, T.; Kakimoto, M.; Imai, Y.; Watanabe, J. *Macromol. Chem. Phys.* **1997**, *198*, 519–530.
- (8) Kaneko, T. I.; Imamura, K.; Watanabe, J. *Macromolecules* **1997**, *30*, 4244–4246.
- (9) Huang, H. W.; Kaneko, T. I.; Horie, K.; Watanabe, J. *Polymer* **1999**, *40*, 3821–3828.
- (10) Costa, G.; Eastmond, G. C.; Fairclough, J. P. A.; Paprotny, J.; Ryan, A. J.; Stagnaro, P. *Macromolecules* **2008**, *41*, 1034–1040.
- (11) Dingemans, T. J.; Mendes, E.; Hinkley, J. J.; Weiser, E. S.; StClair, T. L. *Macromolecules* **2008**, *41*, 2474–2483.
- (12) Shoji, Y.; Higashihara, T.; Watanabe, J.; Ueda, M. *Chem. Lett.* **2009**, *38*, 716–717.
- (13) Shoji, Y.; Ishige, R.; Higashihara, T.; Watanabe, J.; Ueda, M. *Macromolecules* **2010**, *43*, 805–810.
- (14) Coates, D. *Liq. Cryst.* **1987**, *2*, 423–428.
- (15) Watanabe, J.; Hayashi, M.; Tokita, M. *React. Funct. Polym.* **1996**, *30*, 191–196.
- (16) Corsellis, E.; Guillon, D.; Kloess, P.; Coles, H. *Liq. Cryst.* **1997**, *23*, 235–239.
- (17) Saunders, K. *Phys. Rev. E* **2008**, *77*, 061708.
- (18) Saunders, K.; Hernandez, D.; Pearson, S.; Toner, J. *Phys. Rev. Lett.* **2007**, *98*, 197801.
- (19) Saunders, K. *Phys. Rev. E* **2009**, *80*, 011703.